



Sustainable one-pot chemo-enzymatic synthesis of chiral furan amino acid from biomass via magnetic solid acid and threonine aldolase

Lei Gong^{a,b}, Yuansong Xiu^a, Jinjun Dong^{a,c}, Ruizhi Han^a, Guochao Xu^a, Ye Ni^{a,*}

^a Key Laboratory of Industrial Biotechnology, Ministry of Education, School of Biotechnology, Jiangnan University, Wuxi 214122, Jiangsu, China

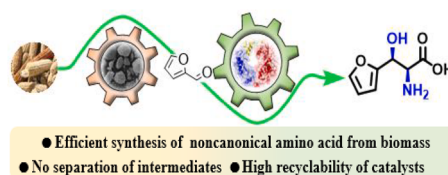
^b Institute of Urban & Rural Mining, National & Local Joint Engineering Research Center on High Efficient Biorefinery and High Quality Utilization of Biomass, Changzhou University, Changzhou 213164, Jiangsu, China

^c Danyang Jindanyang Winery Industry Co., Ltd., Danyang 212300, Jiangsu, China

HIGHLIGHTS

- Magnetic solid acid could catalyze biomass to produce furfural.
- Bio-derived furfural was converted into β -(2-furyl)serine by a L-threonine aldolase.
- One-pot chemo-enzymatic synthesis of ncAA from biomass was established.
- Solid acid and biocatalyst could be efficiently recycled for 5 cycles.

GRAPHICAL ABSTRACT



ARTICLE INFO

Keywords:

Chemo-enzymatic
Magnetic solid acid
Furfural
L-threonine aldolase
 β -(2-furyl)serine

ABSTRACT

Sustainable synthesis of valuable noncanonical amino acids from renewable feedstocks is of great importance. Here, a feasible chemo-enzymatic procedure was developed for the synthesis of chiral β -(2-furyl)serine from biomass catalyzed by a solid acid catalyst and immobilized *E. coli* whole-cell harboring L-threonine aldolase. A novel magnetic solid acid catalyst $\text{Fe}_3\text{O}_4@\text{MCM-41}/\text{SO}_4^{2-}$ was successfully synthesized for conversion of corn cob into furfural in an aqueous system. Under the optimum conditions, furfural yield of 63.6% was achieved in 40 min at 180 °C with 2.0% catalyst (w/w). Furthermore, biomass-derived furfural was converted into an aldol-addition product β -(2-furyl)serine with 73.6% yield, 99% *ee* and 20% *de* by immobilized cells in 6 h. The magnetic solid acid and biocatalyst can be readily recovered and efficiently reused for five consecutive cycles without significant loss on product yields. This chemo-enzymatic route can be attractive for producing noncanonical amino acids from biomass.

1. Introduction

Optically active noncanonical amino acids (nCAAs) have received considerable attention for their diverse biological activities as important pharmaceuticals intermediates, food additives and fine chemicals (Williams, 1992; Servi et al., 2008). Among them, β -(2-furyl)serine (FS) belongs to heterocyclic β -hydroxy- α -amino acids, is known as an important value-added product of furfural, which is found as

constituents in furan antibiotics and as precursors of the fine chemical 2-amino-1-(2-furyl) ethanol. The chemical synthesis of FS usually results in racemic mixtures, and requires large amount of organic solvents at strong alkali condition and around 4 °C, which is environmental unfriendly and often time-consuming (Hayes and Gever, 1951). As a consequence, the development of convenient and green protocols for the production of FS enantiomers has become an important issue.

Furfural, an aldehyde of furan, is generally produced by acid-

* Corresponding author.

E-mail address: yeni@jiangnan.edu.cn (Y. Ni).

<https://doi.org/10.1016/j.biortech.2021.125344>

Received 8 April 2021; Received in revised form 24 May 2021; Accepted 26 May 2021

Available online 29 May 2021

0960-8524/© 2021 Elsevier Ltd. All rights reserved.

catalyzed hydrolysis of hemicellulose-rich biomass such as corn stover, sorghum durra stalk, and corncob. Hemicellulose is a natural polysaccharide consisted of xylose, arabinose, etc. Furfural serves as a pivotal intermediate that bridges bio-based products (e.g. furfurylamines and furfuryl alcohols) and C5 carbohydrates (primarily xylose). Efficient production and comprehensive utilization of bio-based furfural is envisaged to be prospective to achieve sustainable biorefineries (Xia et al., 2018; Shen et al., 2020). Traditional homogeneous catalysts such as mineral acids (mainly H_2SO_4) can be used to produce furfural with steam as stripping agent, however suffer disadvantages of by-products, unrecyclable catalyst, serious pollution, and high-energy consumption (Singh, 2018; Nie et al., 2019; Catrinck et al., 2020). Alternatively, heterogeneous solid acids including metal oxide, amberlyst, zeolites, acid-functionalized MCM materials, sulfonated biochar catalysts, supported metal and heteropoly acids (Peng et al., 2019; Delbecq et al., 2018; Deng et al., 2016), exhibit superior efficacy in furfural production with high activity and selectivity, low equipment corrosion, and excellent reusability than homogeneous catalysts. Although heterogeneous acids can be rapidly separated from liquid-phase reaction media by filtration or centrifugation for recycle, they are not readily separable from solid lignocellulosic biomass in one-pot catalytic reactions. Developing and application of magnetic catalysts is a promising approach to overcome this issue. Due to their unique magnetic and insoluble properties, magnetic catalysts can be separated more easily in the presence of external magnetic field, particularly for solid reaction mixtures (Sudarsanam et al., 2018; Li et al., 2018). Hence, it is of special interest to develop consolidated lignocellulosic biomass conversion strategies to produce furfural employing magnetic-based heterogeneous catalysts.

Recently, various catalysts have been discovered, characterized and utilized in the efficient preparation of furfural derivatives (Zhang et al., 2020; Wang et al., 2020a, 2020b; Yu et al., 2020; Liu et al., 2020). Biocatalysts have many advantages over traditional chemical catalysts for the aldol reaction due to their high catalytic efficiency and specificity as well as mild conditions (Wang et al., 2020a, 2020b; Kurjatschij et al., 2014; Chen et al., 2016). Threonine aldolases (TAs), a class of pyridoxal 5'-phosphate (PLP) dependent enzymes, catalyze the reversible aldol addition of aldehyde with glycine to afford β -hydroxyl- α -amino acids with two new stereogenic centers at α - and β -positions (Wang et al., 2020a, 2020b). According to the stereospecificity at α -carbon, TAs can be classified into L- and D-type. Moreover, β -hydroxyl- α -amino acids can be produced in both *threo* and *erythro* forms that determined by the binding property of the general base to the β -carbon. LTA from *E. coli*, L-*allo*-TA from *T. maritima* and *A. jandaei* have been employed for furfural (100 mM) aldol addition with glycine for the synthesis of FS. However, less than 18% conversion was obtained in all above reactions (Beaudoin et al., 2018), ascribing to the strong inhibitory effect of furfural on enzymes and microbial cells. Furthermore, to the best of our knowledge, there is few reports on one-pot conversion of lignocellulosic biomass into FS via chemical and biological catalysts in tandem.

In this work, an efficient one-pot chemo-enzymatic route was developed to convert lignocellulosic biomass into FS. A core-shell solid acid catalyst, $Fe_3O_4@MCM-41/SO_4^{2-}$, was synthesized to prepare furfural from corncob. *E. coli* whole-cell harboring PpLTA (LTA from *Pseudomonas putida*) were constructed and exhibited excellent aldol addition activity in FS synthesis. In one-pot chemo-enzymatic cascade system, synthesis of chiral FS from corncob via tandem reactions catalyzed by $Fe_3O_4@MCM-41/SO_4^{2-}$ solid acid and recombinant PpLTA cells were achieved under mild conditions. Key reaction parameters were explored to improve the efficiency of the cascade conversion. Finally, magnetic solid acid and immobilized cells were evaluated for recycling in one-pot systems.

2. Materials and methods

2.1. Chemicals, strains and plasmids

Corn cob was purchased from a local straw agricultural products store in (Lianyungang, China) and crushed into powder (60–80 mesh). Coal fly ash (CFA) was provided by Zhengzhou Power Plant (Henan, China). Pyridoxal 5'-phosphate (PLP) was obtained from Sigma-Aldrich (Shanghai, China). Cellulase was supplied by Vland Biotech Group Co., Ltd. (Qingdao, China). $FeCl_3$, $FeCl_2$, $NH_3 \cdot H_2O$, $(NH_4)_2SO_4$, KH_2PO_4 , CTMAB, and furfural were obtained from Sinopharm Group Chemical Reagent Co., Ltd. (Shanghai, China). Other chemicals are of analytical grade and commercially available. Chemical synthesis of D,L-*threo*- β -(2-furyl)serine was conducted according to reported method (Hayes and Gever, 1951).

E. coli strains JM109 and BL21(DE3) preserved in the laboratory were used as hosts for threonine aldolase genes. Plasmid pET28a (Novagen, Germany) was used for gene expression. Recombinant whole-cell catalyst was prepared as previously described (Gong et al., 2021).

2.2. Preparation of $Fe_3O_4@MCM-41/SO_4^{2-}$ solid acid catalyst

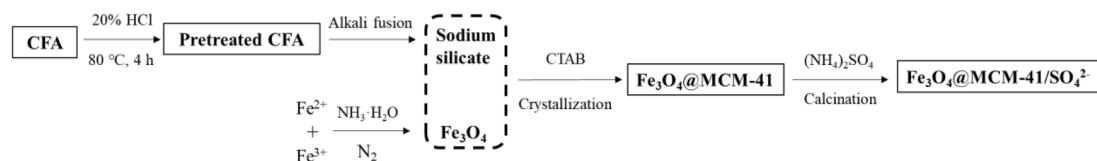
Fe_3O_4 nanoparticles were prepared by chemical co-precipitation of $FeCl_2$ and $FeCl_3$ as described (Xie and Zang, 2016). Raw CFA was pretreated with 20% HCl followed by stirring at 80 °C for 4 h to remove impurities such as iron and calcium, and then filtered, washed and dried to obtain pretreated CFA. Thereafter, sodium hydroxide and pretreated CFA were mixed evenly at a ratio of 1:1.2 (w/w) and then heated in a muffle furnace at 550 °C for 1 h. After alkali fused CFA cooled to room temperature, deionized water was added at a ratio of 1:4 (w/w) and stirred for 24 h. The mixture was subsequently filtered to obtain light yellow solution of sodium silicate, which could be used as a silica source to prepare MCM-41. To synthesize $Fe_3O_4@MCM-41$, the as-prepared Fe_3O_4 was dispersed in deionized water and stirred for 1 h after addition of ammonia. CTAB was dissolved in hot water at a ratio of 1:20 (w/w), and then slowly added to Fe_3O_4 dispersion, followed by stirring for 1 h. The sodium silicate solution was slowly added into the Fe_3O_4 suspension, and stirred continuously for 24 h at 60 °C. The magnetic composite was then hydrothermally treated at 110 °C for 24 h in a reaction kettle after adjusting pH value to 10.5. The solid products were separated by a magnet and washed with deionized water, then dried in an oven at 60 °C overnight. The prepared $Fe_3O_4@MCM-41$ was ground and impregnated in 3.0 M $(NH_4)_2SO_4$ solution at a ratio of 15 mL g^{-1} (v/w) for 24 h. After magnetic separation and drying, solid acid $Fe_3O_4@MCM-41/SO_4^{2-}$ was prepared by calcination at 500 °C for 3 h. The whole process was illustrated in Scheme 1.

2.3. Preparation of immobilized whole-cell biocatalyst

Recombinant *E. coli* strains harboring various LTAs and serine hydroxymethyltransferase (SHMT) were used, including LTA from *Pseudomonas putida* (PpLTA), LTA from *Caulobacter crescentus* (CclTA) and SHMT from *Streptococcus thermophilus*. The immobilized whole-cell biocatalysts were prepared using gelatin (acid-processed) embedding and cross-linking method, based on the previous method and slightly improved (Labus et al., 2016).

2.4. Synthesis of furfural from corncob catalyzed by solid acid $Fe_3O_4@MCM-41/SO_4^{2-}$

General procedure for conversion of corncob into furfural was conducted in a 200-mL stainless steel reactor, which contained 10 g of corncob powder, 100 mL of deionized water and a certain amount of solid acid $Fe_3O_4@MCM-41/SO_4^{2-}$ (0.25–5.0%, w/w). The reaction mixture was stirred at 500 rpm and heated rapidly to specified temperature (160–200 °C), and then held for a certain time period (5–180



Scheme 1. Schematic diagram of the preparation of solid acid catalyst $\text{Fe}_3\text{O}_4@\text{MCM-41}/\text{SO}_4^{2-}$.

min) with mechanical agitation (500 rpm). Afterwards, the reactor was immediately cooled to room temperature by ice bath. The concentration of xylose and furfural was determined by high performance liquid chromatography (HPLC).

2.5. Biocatalytic asymmetric synthesis of FS in a chemo-enzymatic reaction system

The optimal biocatalytic reaction conditions were investigated using commercial furfural (5 mM) as substrate. The effects of various parameters were investigated, including pH (MES buffer, pH 5.0–7.0; HEPES buffer, pH 7.0–9.0; CHES buffer, pH 9.0–10.0; all were 100 mM), temperature (10–60 °C), divalent metal ions (Zn^{2+} , Fe^{2+} , Mn^{2+} , Cu^{2+} , Ni^{2+} , Ca^{2+} , Co^{2+} and Mg^{2+} , 1 mM), cofactor PLP concentration (1–100 μM), furfural concentration (25–300 mM) and recombinant cells (5–60 $\text{g}\cdot\text{L}^{-1}$). Glycine was added at 10-fold to furfural unless other statement, to drive the reaction equilibrium toward FS synthesis.

Bioconversion of corncob derived furfural hydrolysate with *E. coli* PplTA whole-cell (20 $\text{g}\cdot\text{L}^{-1}$) were conducted in the same 200-mL reactor (250 rpm) at 30 °C and pH 8.0.

2.6. Saccharification of solid acid-pretreated corncob residues

Saccharification reaction was performed in 50-mL conical flasks with a working volume of 10 mL. Corncob residues (1 g) was mixed with citrate buffer solution (50 mM, pH 4.8) containing cellulase (40 FPU $\cdot\text{g}^{-1}$ biomass). The mixture was incubated at 50 °C and 120 rpm for 48 h. Samples were withdrawn at 0, 6, 12, 24, 48 h, and the reaction was immediately quenched by heating in a boiling water bath. The hydrolysis products glucose and xylose were determined using HPLC. Raw corncob was used as control.

2.7. Characterization of solid acid catalyst

The characterization procedures of SEM, FT-IR, XRD, BET and EDAX were as previously reported (Gong et al., 2019). Hysteresis regression curves of the sample particles were determined using a vibration sample magnetometer (VSM) system 7407 (Lake Shore, USA) to estimate the magnetic properties of catalyst. In order to further clarify the type and activity of acidic sites on solid acid, the Brønsted and Lewis acidic sites were evaluated by Fourier-transform infrared spectrometry after adsorption of pyridine (Py-IR) (Nexus 470, Thermo Nicolet, USA).

2.8. Analytical methods

The concentrations of reducing sugars (glucose and xylose) were determined by HPLC (Agilent 1260 Infinity, USA) using an Aminex HPX-87H column (300 \times 7.8 mm, Bio-Rad, USA) at 60 °C with a refractive index detector, and 5 mM sulfuric acid (0.5 mL $\cdot\text{min}^{-1}$) was used as the eluent. Furfural concentration was determined by reversed-phase HPLC with a Diamonsil C18 column (250 \times 4.6 mm, Dikma) as previously reported (Gong et al., 2019). Enantiomers and diastereoisomers of FS were determined by HPLC after OPA/NAC pre-column derivatization, with $\text{KH}_2\text{PO}_4\text{-NaOH}$ buffer (50 mM, pH 8.0): acetonitrile (82:18, v/v) as the eluent. The column temperature, detection wavelength and flow rate were 40 °C, 338 nm and 0.8 mL $\cdot\text{min}^{-1}$, respectively. Changes in the chemical composition of corncob before and after solid acid

pretreatment were measured following previous report (Zhang et al., 2016).

3. Results and discussion

3.1. Characterization of magnetic solid acid $\text{Fe}_3\text{O}_4@\text{MCM-41}/\text{SO}_4^{2-}$

Micro-morphology surface of Fe_3O_4 , $\text{Fe}_3\text{O}_4@\text{MCM-41}$ and $\text{Fe}_3\text{O}_4@\text{MCM-41}/\text{SO}_4^{2-}$ was characterized by SEM (see supplementary materials). Fe_3O_4 nanoparticles were synthesized as quasi-spherical particles with uneven surface. Aggregation of particles was observed owing to their magnetic interaction. The spherical shape of the resultant material was retained after coating with MCM-41. Magnetic particles were wrapped by MCM-41, and there was no appreciable change in the shape of the nanoparticles after the surface functionalization.

FT-IR spectra of $\text{Fe}_3\text{O}_4@\text{MCM-41}/\text{SO}_4^{2-}$ was further measured to reveal its microstructure characteristics (see supplementary materials). The absorption peaks at 3440 cm^{-1} and 1629 cm^{-1} corresponded to the stretching and bending vibrations of O–H bonds. The peaks at approximately 1100 cm^{-1} and 881 cm^{-1} were related to Si–O–Si asymmetric and symmetric telescopic vibrations, respectively. The bending vibration at around 460 cm^{-1} belonged to Si–O bond. The characteristic peaks of Fe_3O_4 were observed at 638 cm^{-1} and 595 cm^{-1} . The peaks at 1127 cm^{-1} and 1070 cm^{-1} corresponded to the double coordination adsorption structure of SO_4^{2-} on the catalyst surface, instead of sulfate.

The crystallinity of $\text{Fe}_3\text{O}_4@\text{MCM-41}/\text{SO}_4^{2-}$ was studied by XRD (see supplementary materials). The six main characteristic diffraction peaks were located at $2\theta = 30.12^\circ$, 35.48° , 43.12° , 53.5° , 57.04° and 62.64° , indicating an uncharged face-centered cubic phase and crystal structures of Fe_3O_4 after modification. $\text{Fe}_3\text{O}_4@\text{MCM-41}$ catalyst was transformed from amorphous to crystalline states due to acidification and calcination, corresponding to the characteristic diffraction peaks at 22–30° and 30–35°.

The magnetic properties of $\text{Fe}_3\text{O}_4@\text{MCM-41}/\text{SO}_4^{2-}$ were investigated by VSM (see supplementary materials). The magnetic hysteresis curves of both samples exhibited a typical superparamagnetic feature. The saturation magnetization of Fe_3O_4 and $\text{Fe}_3\text{O}_4@\text{MCM-41}/\text{SO}_4^{2-}$ nanoparticles were determined to be 80 and 46 $\text{emu}\cdot\text{g}^{-1}$ respectively, which were sufficient for phase separation using a conventional magnet. It is speculated that the decrease in saturation magnetization of $\text{Fe}_3\text{O}_4@\text{MCM-41}/\text{SO}_4^{2-}$ was due to the decrease of magnetic content after the coating of non-magnetic MCM-41 on Fe_3O_4 nanoparticles.

The EDAX spectrum of $\text{Fe}_3\text{O}_4@\text{MCM-41}/\text{SO}_4^{2-}$ showed peaks of Fe, O, Si, and S, indicating successful coating and functionalizing of magnetite nanoparticles by MCM-41 and $(\text{NH}_4)_2\text{SO}_4$ (see supplementary materials).

Py-IR spectrum of $\text{Fe}_3\text{O}_4@\text{MCM-41}/\text{SO}_4^{2-}$ showed the acidity of a solid acid (see supplementary materials). Typical peaks of Lewis acid (L) appeared near 1600 cm^{-1} and 1450 cm^{-1} , and the characteristic peak of Brønsted acid (B) appeared at 1540 cm^{-1} , and an overlapping of L and B peaks was detected at 1489 cm^{-1} . The results showed that the solid acid catalyst has the properties of both Brønsted and Lewis acid, and the absorption peak of Lewis acid was significantly higher than that of Brønsted acid, suggesting Lewis acid is much stronger than Brønsted acid.

BET method was used to distinguish the structural characteristics of catalysts. The results showed that the surface area and pore size of Fe_3O_4

were significantly increased after MCM-41 coating and $(\text{NH}_4)_2\text{SO}_4$ acidification, which could facilitate the catalytic efficiency (Table 1).

3.2. Preparation of furfural from corncob by $\text{Fe}_3\text{O}_4@MCM-41/\text{SO}_4^{2-}$ catalyst

The preparation system of furfural was established. Reaction conditions for the production of furfural from corncob were investigated, including catalyst loading (0.25–5.0%, w/w), reaction temperature (160–200 °C) and duration (5–180 min).

Notably, the yields of furfural increased at catalyst loadings of 0.25–2.0% (w/w), and no significant increase was observed at 2.0–5.0% (w/w) catalyst loadings. Therefore, a catalyst loading of 2.0% (w/w) was chosen for further investigation (see supplementary materials). Reaction temperature and duration are important factors in corncob degradation. First, hemicellulose of corncob was hydrolyzed into xylose, and then the obtained xylose was dehydrated to form furfural by solid acid catalyst. Reactions were operated under different temperatures (160–200 °C) and durations (5–180 min), and the concentrations of furfural and xylose were measured (Fig. 1). Initially, an increasing in furfural yield was observed with extended reaction time under various temperatures. After culminated at certain reaction time, furfural concentrations at 180–200 °C gradually declined due to further degradation. The highest furfural concentration of 72 mM was obtained at 180 °C for 40 min. It was also noted that higher temperature was favorable for high furfural yields, while could also accelerate the degradation of furfural with prolonged reaction time. The xylose concentration decreased during the time course under all tested temperatures. Higher reaction temperatures could facilitate depolymerization of corncob hemicellulose and dehydration of xylose. Components of solid acid $\text{Fe}_3\text{O}_4@MCM-41/\text{SO}_4^{2-}$ were also investigated individually as control. The catalytic efficiency of individual components of $\text{Fe}_3\text{O}_4@MCM-41/\text{SO}_4^{2-}$ was also investigated (see supplementary materials). The results indicate synergistic effects of each components in $\text{Fe}_3\text{O}_4@MCM-41/\text{SO}_4^{2-}$ on furfural production. Moreover, under the same acidic condition (pH 2.0), solid acid $\text{Fe}_3\text{O}_4@MCM-41/\text{SO}_4^{2-}$ displayed higher catalytic activity than diluted H_2SO_4 . All above demonstrates that $\text{Fe}_3\text{O}_4@MCM-41/\text{SO}_4^{2-}$ has stronger catalytic active components and higher selectivity than inorganic acid catalysts.

3.3. Conversion of furfural into chiral FS employing recombinant *Ppl*.TA cells

Biocatalysis has become one of the most promising approach in the asymmetric synthesis of fine chemicals due to its mild conditions, outstanding stereoselectivity, and environmental friendliness (Yang et al., 2020; Cheng et al., 2020; Xue et al., 2018). Here, recombinant *E. coli* whole-cell harboring different enzymes including *Ppl*.TA, *Ccl*.TA and SHMT, were constructed for the bioconversion of furfural into chiral β -(2-furyl)serine. Recombinant *Ppl*.TA cells showed the highest furfural aldol addition activity (see supplementary materials). To further enhance its aldol addition activity, effects of reaction pH (5.0–10.0), reaction temperature (10–60 °C), divalent metal ions (Zn^{2+} , Fe^{2+} , Mn^{2+} , Cu^{2+} , Ni^{2+} , Ca^{2+} , Co^{2+} and Mg^{2+}), cofactor PLP concentrations (1–100 μM) on aldol addition reaction were studied separately using recombinant *Ppl*.TA cells. The highest aldol addition activity was obtained at 30

°C, pH 8.0, and 50 μM of PLP without metal ion (Table 2).

As we know, furan aldehydes could negatively affect the catalytic activity of enzyme and microbial cells (Palmqvist and Hahn-Hägerdal, 2000). Therefore, the tolerance of *E. coli Ppl*.TA whole-cell biocatalysts toward different furfural concentrations (25–300 mM) was investigated (Fig. 2a). A complete conversion was observed at furfural concentrations of 25 mM and 50 mM. Further increased in furfural concentrations (75–300 mM) resulted in obvious inhibitory effect. Furfural conversion increased at cell loadings of 5–20 $\text{g}\cdot\text{L}^{-1}$, and no significant change in the conversion at higher cell loading was observed (Fig. 2b). Considering the yield and biocatalyst cost, cell loading of 20 $\text{g}\cdot\text{L}^{-1}$ was chosen.

3.4. Chemo-enzymatic synthesis of chiral FS from biomass-derived furfural in one-pot

Compared with chemical and enzymatic synthesis, chemo-enzymatic tandem reaction is more efficient and economic, which has been applied in the synthesis of many value-added chiral compounds (Pajak et al., 2018; Shen et al., 2008). Chiral FS, a value-added product of furfural, was synthesized from corncob via cascade catalysis with magnetic solid acid $\text{Fe}_3\text{O}_4@MCM-41/\text{SO}_4^{2-}$ and recombinant *E. coli Ppl*.TA in one-pot system. In a 200-mL Teflon tank reactor containing 100 mL aqueous medium (pH 2.0), 10 g of corncob powder was converted into 72 mM furfural catalyzed by solid acid $\text{Fe}_3\text{O}_4@MCM-41/\text{SO}_4^{2-}$ at 180 °C for 40 min. Then, after adjusting pH value to 8.0, 720 mM glycine, 50 μM PLP and 20 $\text{g}\cdot\text{L}^{-1}$ recombinant *E. coli Ppl*.TA whole-cell were added to the same reaction vessel for bioconversion at 30 °C and 200 rpm, without any purification steps. After 6 h of bioconversion, 72 mM corncob-derived furfural was converted into 53 mM FS (Fig. 3) with 99% *ee* and 20% *de* (*threo*) (see supplementary materials). And the bioconversion of commercial furfural at the same concentration was conducted as a control, which exhibited similar reaction curve and conversion ratio (see supplementary materials). Therefore, the chemical reaction system of corncob exhibited good biological compatibility, which could potentially be integrated with biocatalytic synthesis of other valuable amino acid derivatives. For example, biomass-derived carbonyl compounds (such as 5-hydroxymethylfurfural, levulinic acid) could be converted to corresponding valuable ncAAs catalyzed by specific TAs via this chemo-enzymatic system.

Corncob residue and solid acid catalyst were removed from the system after one-pot conversion. The reaction mixture was then extracted with diethyl ether to remove any unreacted furfural. Methanol (400 mL) was added to the aqueous phase obtained from extraction, and incubated at 4 °C overnight to precipitate most of the unreacted glycine. The precipitated glycine was collected and washed with methanol. After evaporating the methanol, the residue was dissolved in phosphate buffer at pH 8.0, and excess glycine oxidase (*Bacillus subtilis* strain 168, UniProt: O31616) was added to decompose any residual glycine (Beaudoin et al., 2018). The aldol product was purified on an anion exchange resin, eluted with 0.5% aqueous acetic acid. The FS product obtained after evaporation was crystallized at 4 °C. The crystalline solid was washed with cold ethanol to give final product as a yellow powder (37.8% yield). It was confirmed as FS by ^1H NMR (400 MHz, D_2O) δ 7.56 (d, $J = 1.8$ Hz, 1H), 6.53–6.46 (m, 2H), 5.29 (d, $J = 4.3$ Hz, 1H), 4.06 (d, $J = 4.3$ Hz, 1H), and ^{13}C NMR (101 MHz, D_2O) δ 171.58, 151.50, 143.49, 110.63, 108.45, 65.63, 58.25 (see supplementary materials).

3.5. Efficient saccharification of solid acid-pretreated corncob

After the reaction, magnetic solid acid was separated from corncob residues for further use. The chemical compositions of corncob residue were analyzed. As shown in Table 3, after solid acid pretreatment, the content of glucan increased from 36% to 46%, and the proportion of xylan decreased from 17% to merely 0.5%. The removal ratios of hemicellulose and lignin were 98% and 36%, respectively. Thus, most of xylan was degraded and part of lignin was removed, which was

Table 1

Pore characterizations of Fe_3O_4 , $\text{Fe}_3\text{O}_4@MCM-41$ and $\text{Fe}_3\text{O}_4@MCM-41/\text{SO}_4^{2-}$.

Sample	BET surface area ($\text{m}^2\cdot\text{g}^{-1}$)	Pore volume ($\text{cm}^3\cdot\text{g}^{-1}$)	Pore size (nm)
Fe_3O_4	5.65	0.014	10.16
$\text{Fe}_3\text{O}_4@MCM-41$	12.65	0.039	12.55
$\text{Fe}_3\text{O}_4@MCM-41/\text{SO}_4^{2-}$	17.95	0.048	10.78

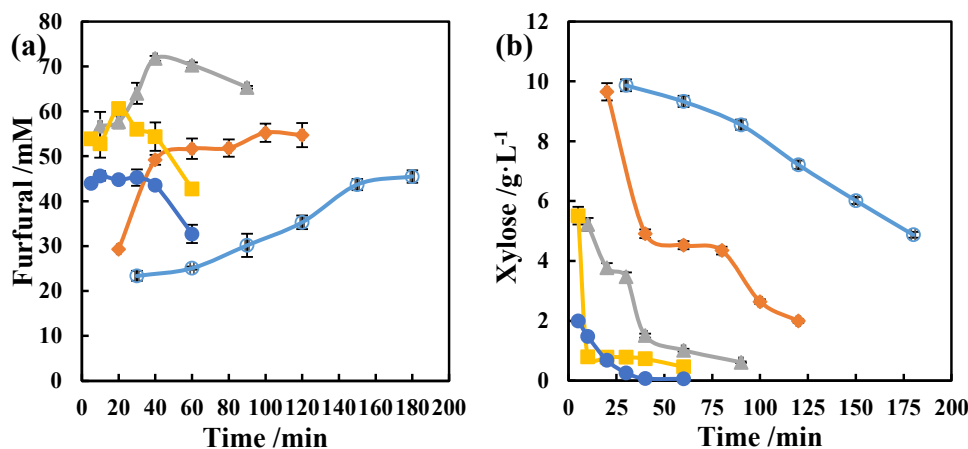


Fig. 1. Effects of reaction temperature and duration on furfural production (a) and xylose concentration (b). Conditions: 10 g raw corncob was mixed with 2.0% (w/w) $\text{Fe}_3\text{O}_4@\text{MCM-41}/\text{SO}_4^{2-}$ and 100 mL deionized water at 160–200 °C for 5–180 min. (○): 160 °C; (◆): 170 °C; (▲): 180 °C; (■): 190 °C; (●): 200 °C.

Table 2

Effects of bioconversion conditions on catalytic activity of recombinant *PpLTA* cells. (a): pH (MES buffer, pH 5.0–7.0; HEPES buffer, pH 7.0–9.0; CHES buffer, pH 9.0–10.0; all were 100 mM); (b): Temperature (10–60 °C); (c): Divalent metal ions types (1 mM); (d): PLP concentration (1–100 μM).

pH ^(a)	Relative activity (%)	Temp. ^(b) (°C)	Relative activity (%)	Metal ions ^(c)	Relative activity (%)	PLP ^(d) (μM)	Relative activity (%)
5	38.7 ± 0.5	10	75.0 ± 1.4	None	100 ± 3.1	1	30.0 ± 0.1
6	50.5 ± 0.8	20	87.8 ± 1.8	Zn ²⁺	67.6 ± 2.3	5	74.0 ± 0.8
7	70.2 ± 1.2	30	100 ± 2.6	Fe ²⁺	67.0 ± 2.5	20	88.0 ± 2.5
7	76.0 ± 1.5	40	76.1 ± 0.9	Mn ²⁺	50.8 ± 1.6	50	99.0 ± 2.7
8	100.0 ± 2.0	50	71.4 ± 1.8	Cu ²⁺	43.1 ± 1.4	100	100.0 ± 2.9
9	92.0 ± 1.2	60	59.3 ± 2.2	Ni ²⁺	41.1 ± 1.9		
9	80.5 ± 1.4			Ca ²⁺	33.5 ± 1.5		
10	62.3 ± 0.9			Co ²⁺	30 ± 0.8		
				Mg ²⁺	29.5 ± 0.2		

Conditions (a): 1 mL of reaction media containing 100 mM buffer solution (pH 5.0–10.0), 50 μM PLP, 5 mM furfural, 50 mM glycine and appropriate amount of recombinant *PpLTA* cells at 30 °C.

Conditions (b): 1 mL of reaction media containing 100 mM HEPES buffer, 50 μM PLP, 5 mM furfural, 50 mM glycine and appropriate amount of recombinant *PpLTA* cells at 10–60 °C and pH 8.0.

Conditions (c): 1 mL of reaction media containing 100 mM HEPES buffer, 50 μM PLP, 5 mM furfural, 50 mM glycine and appropriate amount of recombinant *PpLTA* cells in the presence of divalent metal ions (Zn²⁺, Fe²⁺, Mn²⁺, Cu²⁺, Ni²⁺, Ca²⁺, Co²⁺, Mg²⁺) at 30 °C and pH 8.0.

Conditions (d): 1 mL of reaction media containing 100 mM HEPES buffer, 1–100 μM PLP, 5 mM furfural, 50 mM glycine and appropriate amount of recombinant *PpLTA* cells at 30 °C and pH 8.0.

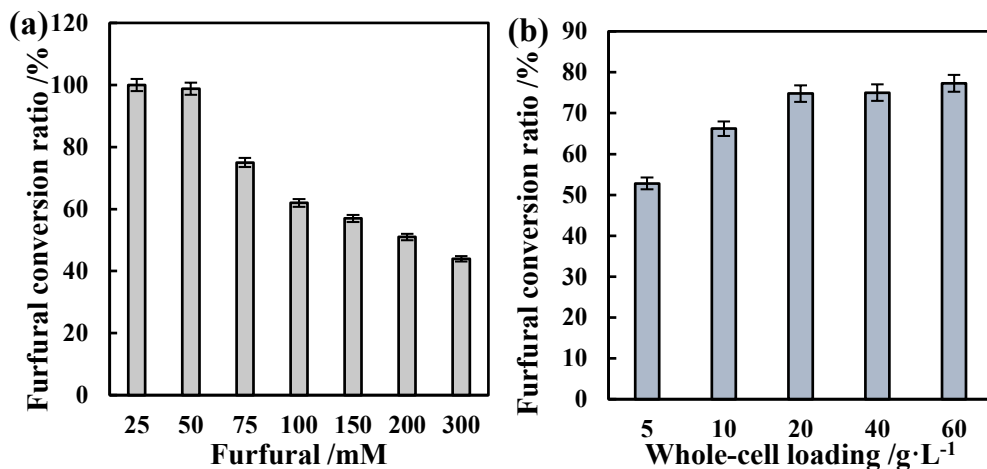


Fig. 2. Effects of various furfural concentration (25–300 mM) on whole-cell bioconversion (a). Condition: 1 mL of reaction media containing 100 mM HEPES buffer, 25–300 mM furfural, 250–3000 mM glycine, 50 μM PLP and 20 g·L⁻¹ wet cells at 30 °C and pH 8.0 for 6 h. Effects of whole-cell loading (5–60 g·L⁻¹) on bioconversion (b). Conditions: 1 mL of reaction media containing 100 mM HEPES buffer, 75 mM furfural, 750 mM glycine, 50 μM PLP and 5–60 g·L⁻¹ wet cells at 30 °C and pH 8.0 for 6 h.

conductive to the enzymatic hydrolysis of corncob residue. Remarkably, the concentration of glucose obtained from corncob pretreated with solid acid was significantly higher than from raw corncob (Fig. 4). Using 40 FPU·g⁻¹ biomass, 45 g·L⁻¹ glucose was achieved from pretreated

corncob at 48 h, which was about 2.5-fold of that of raw material. Moreover, extremely low xylose (less than 2 g·L⁻¹) was detected due to the degradation of hemicellulose into furfural.

To understand the high glucose yield in hydrolysis, the morphology

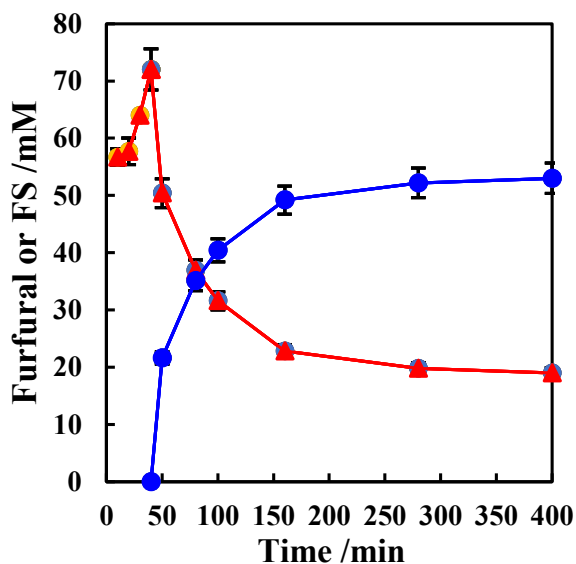


Fig. 3. Time courses of chemo-enzymatic tandem conversion of corncob to produce FS via pretreatment with solid acid $\text{Fe}_3\text{O}_4@\text{MCM-41}/\text{SO}_4^{2-}$ at 180 °C for 40 min and bioconversion with recombinant *PpLTA* cells at 30 °C and pH 8.0. (▲): Furfural; (●): FS.

changes of corncob after solid acid pretreatment was analyzed. After pretreatment, the surface of corncob became rough and loose, with more pores (see supplementary materials), which facilitated the accessibility of cellulase to cellulose. Furthermore, FT-IR spectra of raw and pretreated corncob were also compared (see supplementary materials). Characteristic peaks of hemicellulose were observed at 1737 cm^{-1} and 1243 cm^{-1} , belonging to functional groups of C = O conjugate bond and C-O bond in xylan. After pretreatment, reduction of these two peaks indicate the degradation of hemicellulose in corncob residues. The characteristic peak of β -1,4-glucosidic bond was obviously weakened at 890 cm^{-1} , suggesting destroyed and degraded cellulose chain. The band at 1515 cm^{-1} represents absorption peak of benzene ring in lignin, which was not detected in corncob residue indicating it was also destroyed. Above data further proved that the magnetic solid acid pretreatment was effective in improving enzymatic hydrolysis of cellulose.

3.6. Recycling of magnetic solid acid catalyst and immobilized biocatalyst

Recycling of catalysts is essential to meet the requirement of green and sustainable chemistry (Manzoli et al., 2019; Mogharabi-Manzari et al., 2019). Reusability of solid acid and immobilized whole-cell biocatalyst was examined for converting corncob into FS in one-pot process. In a 200-mL stainless steel reactor, corncob powder (60–80 mesh, 10 g) was evenly mixed in 100 mL of deionized water containing $\text{Fe}_3\text{O}_4@\text{MCM-41}/\text{SO}_4^{2-}$ solid acid (2.0%, w/w, pH 2.0) at 180 °C and 500 rpm for 40 min. After adjusting the pH value to 8.0, the immobilized biocatalysts (equivalent to 20 $\text{g}\cdot\text{L}^{-1}$ wet cells) were added into furfural reactor for bioconversion. The bioconversion was allowed to continue for 6 h at 30 °C. Magnetic solid acid could be facily separated and recovered from the reaction system by magnetic force, and the immobilized cells were recovered by easy filtration. The recovered immobilized cells were rinsed with saline for the next bioconversion batch.

Table 3

Compositions of corncob and residue after magnetic solid acid pretreatment.

Corn-cob	Contents (%)			Removal rates (%)		Recovery (%)
	Glucan	Xylan	Lignin	Hemicellulose	Lignin	Solid
Raw	36	17	33	–	–	100
Pretreated	46	0.5	34	98	36	62

$\text{Fe}_3\text{O}_4@\text{MCM-41}/\text{SO}_4^{2-}$ solid acid was washed with deionized water and ethanol, then dried in an oven at 60 °C overnight. The recovered catalyst was then impregnated in 3.0 M $(\text{NH}_4)_2\text{SO}_4$ for 24 h again before calcining. The recycled $\text{Fe}_3\text{O}_4@\text{MCM-41}/\text{SO}_4^{2-}$ solid acid catalyst and immobilized cells were evaluated in the next batches.

To investigate the stability of $\text{Fe}_3\text{O}_4@\text{MCM-41}/\text{SO}_4^{2-}$ solid acid, the catalyst was applied for 5 continuous batches in one-pot process. Furfural reached 72 mM in 1st batch, and dropped to 62 mM in 5th batch, indicating the solid acid catalyst could maintain 86% of activity and has a stable recyclability. The immobilized cells exhibited good reusability. Using furfural prepared from corncob via recovered solid acid catalyst, furfural conversion of 62.5% was obtained in 5th cycle, which was merely 11.1% lower than that of 1st bath (73.6%). Overall, both magnetic solid acid and immobilized cells exhibited fine stability and reusability in the one-pot chemo-enzymatic synthesis of chiral FS from corncob.

4. Conclusions

Preparation of chiral FS from biomass was performed by magnetic solid acid $\text{Fe}_3\text{O}_4@\text{MCM-41}/\text{SO}_4^{2-}$ and recombinant *PpLTA* cells. A one-pot two-step sequential chemo-enzymatic process was successfully developed, for the first time, to convert biomass directly into chiral FS, a nAA, with simple separation of solid acid and biocatalyst. This strategy allowed minimized isolation of intermediates, thus reduced operation time and waste, and enhanced overall selectivity and yield. Therefore, this work demonstrates the feasibility of chemo-enzymatic transformation of lignocellulosic biomass into chiral furan amino acid. This process could potentially be developed for high-value utilization of corncob to produce biobased amino acid derivatives.

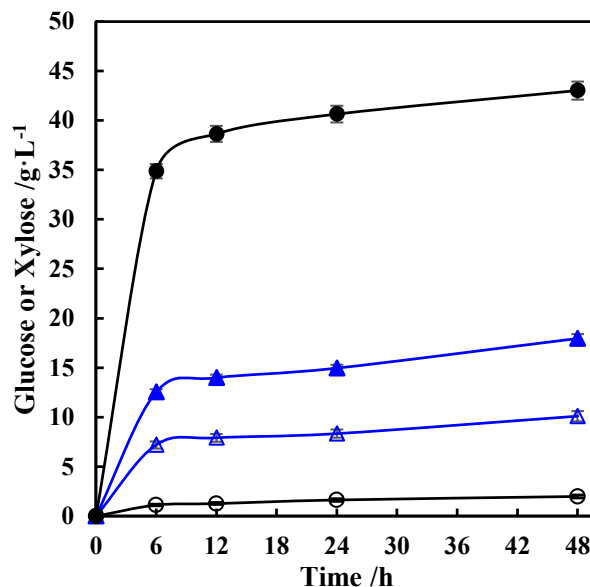


Fig. 4. Enzymatic hydrolysis process of raw corncob and pretreated corncob. Conditions: 10 mL of reaction media containing 50 mM citrate buffer (pH 4.8), cellulase (40 $\text{FPU}\cdot\text{g}^{-1}$ biomass), 1.0 g of raw corncob or pretreated corncob at 50 °C. (●): Glucose in pretreated corncob; (○): Xylose in pretreated corncob; (▲): Glucose in raw corncob; (△): Xylose in raw corncob.

CRedit authorship contribution statement

Lei Gong: Conceptualization, Investigation, Methodology, Visualization, Validation, Writing - original draft. **Yuansong Xiu:** Formal analysis, Visualization, Investigation. **Jinjun Dong:** Resources, Methodology. **Ruizhi Han:** Resources. **Guochao Xu:** Resources, Visualization, Writing - review & editing. **Ye Ni:** Resources, Funding acquisition, Supervision, Writing - review & editing.

Declaration of Competing Interest

The authors declare that they have no known competing financial interests or personal relationships that could have appeared to influence the work reported in this paper.

Acknowledgments

The authors are grateful to the National Key Research and Development Program (2018YFA0901700, 2019YFA0906400), the National Natural Science Foundation of China (22077054, 22078127, 21776112), Postgraduate Research & Practice Innovation Program of Jiangsu Province (KYCX191834), the national first-class discipline program of Light Industry Technology and Engineering (LITE2018-07), and the Program of Introducing Talents of Discipline to Universities (111-2-06) for the financial support of this research.

Data Availability

All data included in this study are available upon request by contact with the corresponding author.

Appendix A. Supplementary data

Supplementary data to this article can be found online at <https://doi.org/10.1016/j.biortech.2021.125344>.

References

- Beaudoin, S.F., Hanna, M.P., Ghiviriga, I., Stewart, J.D., 2018. Progress in using threonine aldolases for preparative synthesis. *Enzyme Microb. Tech.* 119, 1–9.
- Catrinck, M.N., Barbosa, P.S., Filho, H.R.O., Monteiro, R.S., Barbosa, M.H.P., Ribas, R.M., Teófilo, R.F., 2020. One-step process to produce furfural from sugarcane bagasse over niobium-based solid acid catalysts in a water medium. *Fuel Process. Technol.* 207, 106482. <https://doi.org/10.1016/j.fuproc.2020.106482>.
- Chen, Q., Han, L., Chen, X.i., Cui, Y., Feng, J., Wu, Q., Zhu, D., 2016. A sialic acid aldolase from *Peptoclostridium difficile* NAP08 with 4-hydroxy-2-oxo-pentanoate aldolase activity. *Enzyme Microb. Tech.* 92, 99–106.
- Cheng, A.-D., Shi, S.-S., Li, Y., Zong, M.-H., Li, N., 2020. Biocatalytic oxidation of biobased furan aldehydes: Comparison of toxicity and inhibition of furans toward a whole-cell biocatalyst. *ACS Sustain. Chem. Eng.* 8 (3), 1437–1444.
- Delbecq, F., Wang, Y. T., Muralidhara, A., El Ouardi, K., Marlair, G., Len, C., 2018. Hydrolysis of hemicellulose and derivatives—A review of recent advances in the production of furfural. *Front. Chem.*, 6, 146.
- Deng, Aojie, Lin, Qixuan, Yan, Yuhuan, Li, Huiling, Ren, Junli, Liu, Chuanfu, Sun, Runcang, 2016. A feasible process for furfural production from the pre-hydrolysis liquor of corncob via biocatalysts in a new biphasic system. *Bioresour. Technol.* 216, 754–760.
- Gong, Lei, Xu, Guochao, Cao, Xudong, Han, Ruizhi, Dong, Jinjun, Ni, Ye, 2021. High-throughput screening method for directed evolution and characterization of aldol activity of D-threonine aldolase. *Appl. Biochem. Biotechnol.* 193 (2), 417–429.
- Gong, Lei, Xu, Zi-Yan, Dong, Jin-Jun, Li, Hao, Han, Rui-Zhi, Xu, Guo-Chao, Ni, Ye, 2019. Composite coal fly ash solid acid catalyst in synergy with chloride for biphasic preparation of furfural from corn stover hydrolysate. *Bioresour. Technol.* 293, 122065. <https://doi.org/10.1016/j.biortech.2019.122065>.
- HAYES, KENYON, GEVER, GABRIEL, 1951. The preparation of 1-(2-furyl)-2-amino-1,3-propanediol and derivatives. *J. Org. Chem.* 16 (2), 269–278.
- Kurjatschij, Sandra, Katzberg, Michael, Bertau, Martin, 2014. Production and properties of threonine aldolase immobilisates. *J. Mol. Catal. B-Enzym.* 103, 3–9.
- Labus, K., Drozd, A., Trusek-Holownia, A., 2016. Preparation and characterisation of gelatine hydrogels predisposed to use as matrices for effective immobilisation of biocatalysts. *Chem. Pap.* 70, 523–530.
- Li, H.L., Wang, Y.Q., Zhu, Y.K., Xu, X.J., Wu, A.M., Deng, X.M., 2018. Bamboo-derived magnetic carbonaceous solid acid catalyst for the conversion of corncob into furfural promoted by warm water immersion. *Bioresour. Technol.* 237, 6221–6237.
- Liu, Ping, Sun, Luyang, Jia, Xinxin, Zhang, Chen, Zhang, Wei, Song, Yongji, Wang, Hong, Li, Cuiqing, 2020. Efficient one-pot conversion of furfural into 2-methyltetrahydrofuran using non-precious metal catalysts. *Mol. Catal.* 490, 110951.
- Manzoli, Maela, Gaudino, Emanuela Calcio, Cravotto, Giancarlo, Tabasso, Silvia, Baig, R. B. Nasir, Colacino, Evelina, Varma, Rajender S., 2019. Microwave-assisted reductive amination with aqueous ammonia: Sustainable pathway using recyclable magnetic nickel-based nanocatalyst. *ACS Sustain. Chem. Eng.* 7 (6), 5963–5974.
- Mogharabi-Manzari, Mehdi, Ghahremani, Mohammad Hossein, Sedaghat, Tabassom, Shayan, Fatemeh, Faramarzi, Mohammad Ali, 2019. A laccase heterogeneous magnetic fibrous silica-based biocatalyst for green and one-pot cascade synthesis of chromene derivatives. *Eur. J. Org. Chem.* 2019 (8), 1741–1747.
- Nie, Yifan, Hou, Qidong, Li, Weizun, Bai, Chuanyunlong, Bai, Xinyu, Ju, Meiting, 2019. Efficient synthesis of furfural from biomass using SnCl₄ as catalyst in ionic liquid. *Molecules* 24 (3), 594.
- Pajak, Małgorzata, Patka, Katarzyna, Winnicka, Elżbieta, Kańska, Marianna, 2018. The chemo-enzymatic synthesis of labeled L-amino acids and some of their derivatives. *J. Radioanal. Nucl. Ch.* 317 (2), 643–666.
- Palmqvist, Eva, Hahn-Hägerdal, Bärbel, 2000. Fermentation of lignocellulosic hydrolysates II: Inhibitors and mechanisms of inhibition. *Bioresour. Technol.* 74 (1), 25–33.
- Peng, Bo, Ma, Cui-Luan, Zhang, Peng-Qi, Wu, Chang-Qing, Wang, Zi-Wei, Li, Ai-Tao, He, Yu-Cai, Yang, Bin, 2019. An effective hybrid strategy for converting rice straw to furoic acid by tandem catalysis via Sn-sepiolite combined with recombinant *E. coli* whole cells harboring horse liver alcohol dehydrogenase. *Green Chem.* 21 (21), 5914–5923.
- Servi, S., Tessaro, D., Pedrocchi-Fantoni, G., 2008. Chemo-enzymatic deracemization methods for the preparation of enantiopure non-natural alpha-amino acids. *Coord. Chem. Rev.* 252, 715–726.
- Shen, Guanfei, Andrioletti, Bruno, Queneau, Yves, 2020. Furfural and 5-(hydroxymethyl) furfural: Two pivotal intermediates for bio-based chemistry. *Curr. Opin. Green Sust.* 26, 100384.
- Shen, Zhi-Liang, Zhou, Wei-Juan, Liu, Ya-Ting, Ji, Shun-Jun, Loh, Teck-Peng, 2008. One-pot chemoenzymatic syntheses of enantiomerically-enriched O-acetyl cyanohydrins from aldehydes in ionic liquid. *Green Chem.* 10 (3), 283.
- Singh, S.K., 2018. Heterogeneous bimetallic catalysts for upgrading biomass-derived furans. *Asian J. Org. Chem.* 7 (10), 1901–1923.
- Sudarsanam, P., Zhong, R.Y., Van den Bosch, S., Coman, S.M., Parvulescu, V.I., Sels, B.F., 2018. Functionalised heterogeneous catalysts for sustainable biomass valorization. *Chem. Soc. Rev.* 47, 8349–8402.
- Wang, Chenguang, Liu, Yong, Cui, Zhibing, Yu, Xiaohu, Zhang, Xinghua, Li, Yuping, Zhang, Qi, Chen, Lungang, Ma, Longlong, 2020a. In situ synthesis of Cu nanoparticles on carbon for highly selective hydrogenation of furfural to furfuryl alcohol by using pomelo peel as the carbon source. *ACS Sustain. Chem. Eng.* 8 (34), 12944–12955.
- Wang, Li-Chao, Xu, Lian, Xu, Xin-Qi, Su, Bing-Mei, Lin, Juan, 2020b. An L-threonine aldolase for asymmetric synthesis of β-hydroxy-α-amino acids. *Chem. Eng. Sci.* 226, 115812.
- Williams, R.M., 1992. Asymmetric syntheses of α-amino acids. *Aldrichim. Acta.* 25, 11–25.
- Xia, Haiyan, Xu, Siqian, Hu, Hong, An, Jiahuan, Li, Changzhi, 2018. Efficient conversion of 5-hydroxymethylfurfural to high-value chemicals by chemo- and bio-catalysis. *RSC Adv.* 8 (54), 30875–30886.
- Xie, W., Zang, X., 2016. Immobilized lipase on core-shell structured Fe₃O₄/MCM-41 nanocomposites as a magnetically recyclable biocatalyst for interesterification of soybean oil and lard. *Food Chem.* 194, 1283–1292.
- Xue, Ya-Ping, Cao, Cheng-Hao, Zheng, Yu-Guo, 2018. Enzymatic asymmetric synthesis of chiral amino acids. *Chem. Soc. Rev.* 47 (4), 1516–1561.
- Yang, Dong, Ma, Cuiluan, Peng, Bo, Xu, Jianhe, He, Yu-Cai, 2020. Synthesis of furoic acid from biomass via tandem pretreatment and biocatalysis. *Ind. Crop Prod.* 153, 112580.
- Yu, Z.J., Tian, H.L., Sun, K., Shao, Y.W., Zhang, L.J., Zhang, S., Duan, P.G., Liu, Q., Niu, S. L., Dong, D.H., Hu, X., 2020. Impacts of externally added Bronsted and Lewis acid on conversion of furfural to cyclopentanone over Ni/SiC catalyst. *Mol. Catal.* 496, 111187.
- Zhang, L.B., Pu, Y.Q., Cort, J.R., Ragauskas, A.J., Yang, B., 2016. Revealing the molecular structure transformation of hardwood and softwood in dilute acid flowthrough pretreatment. *ACS Sustain. Chem. Eng.* 4, 6618–6628.
- Zhang, Xue-Ying, Wang, Xin, Li, Nan-Wei, Guo, Ze-Wang, Zong, Min-Hua, Li, Ning, 2020. Furan carboxylic acids production with high productivity by cofactor-engineered whole-cell biocatalysts. *Chem. Cat. Chem.* 12 (12), 3257–3264.